Journal Name

Layered double hydroxides anchored ionic liquids as amphiphilic heterogeneous catalysts for Knoevenagel condensation reaction

Tengfei Li,[a] Wei Zhang,[a] Wei Chen,[a] Haralampos N. Miras[b]* and Yu-Fei Song[ac]*

In recent years, great attention has been dedicated to the development of heterogeneous base catalysts rendering green and sustainable process in benign aqueous media. Herein, the ionic liquids modified layered double hydroxides (LDHs) based catalysts of LDH-ILs-Cn (n = 4, 8, 12) were prepared by adopting an exfoliation/assembly strategy, in which the ionic liquids (ILs) was convalently anchored on the surface of LDHs layers. The resultant LDH-ILs-Cn were charaterized by FT-IR, the solid-state ^{13}C NMR, ^{29}Si CP/MAS NMR, ^{27}Al-MAS NMR, XRD, TG-DTA, BET, XPS, SEM, CO_2-TPD and contact angle experiments etc. The catalytic performance of LDH-ILs-C12 for Knoevenagle condensation of a variety of aldehydes with ethyl cyanoacetate/malononitrile in H_2O at room temperature showed excellent yields and selectivity. Moreover, the base catalyst of LDH-ILs-C12 can be easily recycled and reused for at least 5 times without decrease of its catalytic efficiency. The scaled-up experiments revealed that the catalyst retained its efficiency and robustness.

1. Introduction

Knoevenagel reaction between an aldehyde/ketone and active methylene-containing compounds is one of the most significant reactions for the C-C bonds formation,[1-3] which has been applied to synthesize important intermediates or products for perfumes, pharmaceuticals and calcium antagonists.[4-6] Generally, this reaction employs a homogeneous base catalyst such as ammonia, ammonium salts, urea, pyridine, primary and secondary amines.[7-9] Unfortunately, these homogeneous catalysts are difficult to be separated and recycled, which restrict their application in practice. To overcome these problems, development of novel heterogeneous base catalysts have attracted great interest and wide attention during past decades, such as aminopropyl-functionalized SBA-15,[10] nitride zeolites,[11] metal-organic frameworks,[12] SiO_2@LDH.[13] However, these catalytic systems still suffer from the following problems: 1) toxic organic solvents or additives, such as toluene, cyclohexane used are highly corrosive, carcinogenic and require frequent laborious workup treatments; 2) partial blockage of the pores, sintering or fusion into a bulk phase and the possible leaching of the basic components into the reaction mixture; 3) poor accessibility of the reactant and catalytic active sites. Consequently, it is of great urgency to design efficient, recyclable, sustainable and eco-friendly heterogeneous base catalytic system for the Knoevenagel reactions.

Layered double hydroxides (LDHs) are composed of brucite-like two-dimensional sheets and interlayer anions. The chemical formula is generally represented as $[M_{1-x}^{2+}M_x^{3+}(OH)_2]^{x+}[A_{x/n}]^{n-} \cdot mH_2O$,[14-16] where M^{2+} and M^{3+} are di- and trivalent metal cations, A^{n-} is the counterion, and x=0.17-0.33 is defined by the $M^{3+}/(M^{2+}+M^{3+})$ ratio.[17] Each hydroxyl group in the LDHs layers is oriented toward the interlayer region and may be hydrogen bonded to the interlayer anions and water molecules. LDHs are very attractive systems due to its fascinating properties that can be finely tuned by appropriate choice of the composition metal ions, functional guest anions and so on.[18] Therefore, LDHs materials have been successfully applied in various fields, including as adsorption materials, additives in polymers, precursors for functional materials, and in pharmaceutics, photo-chemistry and electrochemistry.[19] In addition, by virtue of the abundance of hydroxyl groups, LDHs are potential solid base catalysts for a wide variety of organic transformations.[14] As solid base catalyst, the base properties of LDHs can be tuned by the composition of metal hydroxide and type of interlayer anions. Moreover, LDHs can be transformed to Lewis acidic and basic bifunctional metal composite oxides by calcination.[13] LDHs are cost-effective, environmentally benign and easy to scaled-up in practice. As a result, LDHs are attracting increasing attention from the viewpoint of environmental and economic concerns.[20]

Ionic liquids (ILs) have been attracted considerable attention owing to their unique properties. For example, nonvolatility, remarkable dissolution, high thermal stability, good catalytic activity, electrophilic/nucleophilic dual activation et al.[21-23] Therefore, ILs has been emerged as good alternatives environmental benign solvents and media to exhibit a rate acceleration effect on catalytic reactions. However, the bottleneck associated with ILs is the difficulty in product isolation and catalyst separation in many circumstances. Moreover, high viscosity of ILs exhibits serious limitation in their practice of industrial catalysts due to the controlled mass transport, which is one of the significant properties in the heterogeneous catalytic system.[24] Thus, the

concept of heterogenization of ILs is being established, which combine the advantages of ILs and appropriate support.[24]

In this paper, we demonstrate the successful preparation of novel heterogeneous base catalysts of LDH-ILs-Cn (n=4,8,12) by covalently grafting onto LDHs layers. Catalytic tests for Knoevenagel condensation in water under room temperature show that among three amphiphilic solid base catalysts, LDH-ILs-C12 exhibits high activity and selectivity, coupled with easy recovery and steady reuse. The sustainable performance and stability during the scaled-up catalytic experiments as well as the cost-effective advantages demonstrate the potential of LDHs-ILs-C12 for industrial applications.

2. Experimental

2.1 Chemical Materials

All chemicals were of analytical grade and were used as received without any further purification. $Mg(NO_3)_2 \cdot 6H_2O$, $Al(NO_3)_3 \cdot 9H_2O$, and hexamethylenetetramine were obtained from Energy Chemical in Shanghai. Ethanol and diethyl ether were purchased from Beijing Chemical Company. Ethyl cyanoacetate (98%), malononitrile (97%), benzaldehyde (98%) and other aldehydes were purchased from Alfa Aesar. LDH-CO_3, LDH-NO_3, [25] 1-butyl-3-(3-triethoxy-silylpropyl)-4,5-dihydro-
imidazolium bromide (ILs-C4), 1-octyl-3-(3-triethoxy-silylpropyl)
-4,5-dihydroimidazolium bromide (ILs-C8), 1-dodelyl-3-(3-triethoxy-silylpropyl)-4,5-dihydroimidazolium bromide (ILs-C12)[26] were synthesized and characterized in accordance with the literature.

2.2. Synthesis of LDH-ILs-Cn (n=4, 8, 12)

In a typical experiment, LDH-NO_3 (0.3 g) was added to formamide (300 mL) in a three necked flask, which was purged with N_2 to avoid carbonate contamination. The mixture was vigorously stirred for 2 days. The mixture was then centrifuged for 10 min and the suspension was isolated by filtration. ILs-Cn (2.6 mmol, n=4, 8, 12) was dissolved in CH_3CN (5 mL) and added dropwise to the above suspension. The reaction mixture was stirred under N_2 for 24 h. 2 g Na_2CO_3 was dissolved in 5 ml H_2O and added dropwise to the reaction mixture. After stirring for 30 min, the resultant precipitate of LDH-ILs-Cn (n=4, 8, 12) was collected by centrifugation and washed with ethanol and water, and dried under vacuum overnight.

2.3 Catalytic test

In a typical Knoevenagel reaction experiment, a mixture of 1 mmol benzaldehyde (or various aldehyde), 1.5 mmol methylene compound (ethyl cyanoacetate or malononitrile), 500 μL H_2O and 30 mg catalyst LDH-ILs-C12 were added into a 10 mL glass bottle at room temperature and the reaction mixture was kept under vigorous stirring. The resulting products were extracted with diethyl ether, analysed by GC and identified by ^{1}H-NMR and ^{13}C-NMR spectroscopy. The yields were calculated by applying reference standards. After

completion of the reaction, the catalyst was recovered by centrifugation, washed with acetone, and dried in vacuum.

3. Results and discussion

3.1. Structural characterization

As shown in Fig 1A, FT-IR spectra of LDH-CO_3 and LDH-ILs-Cn (n=4, 8, 12) show the broad band at 3400-3700 cm^{-1} that can be attributed to the Mg/Al-OH/H_2O vibration. Additionally, the broad peaks from 788 to 449 cm^{-1} can be assigned to the O-M-O (M = Mg or Al) vibration in the brucite-like layers of the LDHs.[27] The strong peak at 1370 cm^{-1} is attributed to C-O anti-symmetric stretching of the interlayer CO_3 anion.[28] Taking LDH-ILs-C12 as an example, it exhibits the C-H stretching bands at 2929 and 2835 cm^{-1} due to the alkyl chain -CH_2 and -CH_3 groups, and a C=N stretching band at 1668cm^{-1} by the imidazole moieties of ionic liquids.[26] Moreover, it shows the characteristic peak at 1060 cm^{-1}, which is assigned to the vibration of the Si-O-M bond (M=Al or Mg).[29] The results indicate that the ionic liquids have been successfully grafted onto the LDHs layers.

As shown in Fig. 1B, the ^{29}Si CP/MAS NMR spectra have been used to investigate the local environment of Si species. For example, the LDHs-ILs-C12 displays three resonance peaks at -65, -59 and -53 ppm that correspond to tridentate, bidentate and monodentate ligation, respectively. The tridentate form implies that all three of the ethoxyl group of ILs-C12 are hydrolysed and condensed with the surface hydroxyl group of LDHs layer. Observation of the bidentate and monodentate form suggest that some ILs-C12 species possess one or two ethoxyl/hydroxyl groups that do not
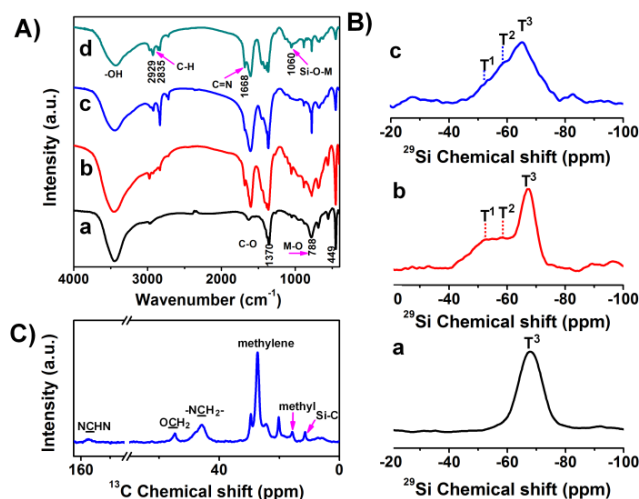

Fig. 1. A) FT-IR spectra of : a) LDH-CO_3, b) LDH-ILs-C4, c) LDH-ILs-C8, d) LDH-ILs-C12; B) Solid-state ^{29}Si CP/MAS NMR spectra of a) LDHs-IL-C4; b) LDHs-IL-C8; c) LDH-ILs-C12; C) Solid-state ^{13}C CP/MAS NMR spectrum of LDH-ILs-C12.
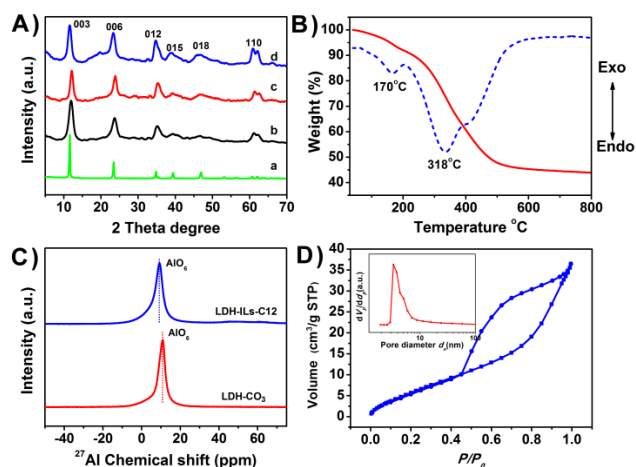
Fig. 2. A) XRD patterns of a) LDH-CO$_3$, b) LDH-ILs-C4, c) LDH-ILs-C8, d) LDH-ILs-C12; B) TG-DTA profile of LDH-ILs-C12; C) The ^{27}Al-MAS-NMR spectra of LDH-CO$_3$ and LDH-ILs-C12. D) The N$_2$ adsorption-desorption isotherm and the pore size distribution (inset picture) of LDH-ILs-C12.

Fig. 3. a) XPS spectrum of the LDH-ILs-C12 sample and deconvolution of the peaks for b) Mg1s, c) Al2p, d) C1s, e) Si2p, f) N1s.

hydrolyze or condense.[30] These results confirm that the ILs-C12 is covalently tethered onto the LDHs layers, resulting in the formation of Al-O-Si and/or Mg-O-Si bonds in the LDHs layers. Fig. 1C shows the solid-state ^{13}C CP/MAS NMR spectrum of LDH-ILs-C12. The spectrum exhibits signals at 154.7, 54.8, 43.1-50.5, 19.9-30.9, 14.7-16.4, and 11.5 ppm that can be assigned to the NCHN, OCH$_2$, -NCH$_2$-, methylene, methyl and Si-C, respectively.[30,31] These signal positions are similar to that the ionic liquids covalently anchored onto SiO$_2$.[31] As a result, the condensation reaction between the hydroxyl groups of LDH layer and ethoxy groups of ionic liquids leads to the formation of covalent Si-O-M (M=Al or Mg) linkage and the maintenance of the dihydroimidazolium skeleton of ionic liquids at the same time.

As shown in Fig. 2A, XRD patterns show the characteristic reflection of LDH-CO$_3$. For LDH-ILs-Cn (n=4, 8, 12), upon modification of ILs, no distinct changes in the refection are observed. In addition, we do not observe a change in the interlayer spacing after silylation, which may be reflected by a shift in d_{003} to lower 2ϑ values.[32] The retention of characteristic peak (110) around $2\vartheta= 60°$ [33] indicates that the structure of the layer has been retained after exfoliation and assembly synthesis.

Thermogravimetric differential thermal analysis (TG-DTA) of LDH-ILs-C12 shows two weight-loss stages as the temperature increasing from 30 to 800 °C (Fig. 2 B). The first weight loss of 8.86 % between 30 °C and 200 °C can be ascribed to the removal of water molecules absorbed on the surface and the interlayer space. The second weight loss of 47.1% between 200 °C and 650 °C corresponds to the decomposition of ILs and subsequent disintegration of the layered structure. Base on the TG-DTA, ICP-AES and elemental analysis (Mg= 18.28 wt %, Al=6.80 wt %, N=1.03 wt %, ILs-C12= 13.03 wt. %), the molecular formula the can be identified as: Mg$_{0.75}$Al$_{0.25}$[O$_3$SiC$_{18}$H$_{36}$N$_2$]$_{0.036}$[Br]$_{0.036}$ (OH)$_{1.92}$[CO$_3$]$_{0.175}$·0.83H$_2$O. The molecular formula of LDH-ILs-Cn (n = 4, 8, 12) is summarized in Table S1, respectively. The thermal stability of
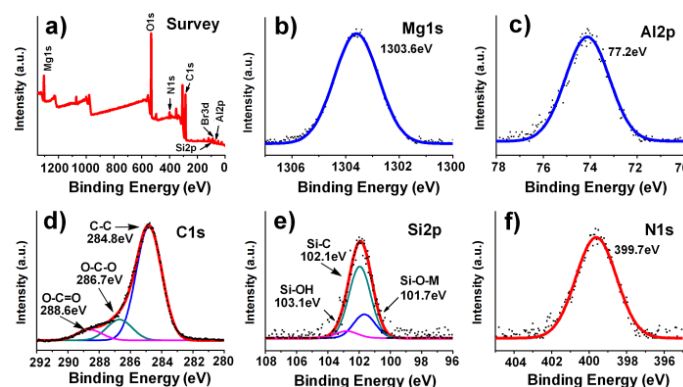
LDH-ILs-C4 and LDH-ILs-C8 are similar to that of the LDH-ILs-C12 (Fig. S1-2). The TG analysis plots of LDH-CO$_3$ are shown in the Figure S3 for comparison.

Solid-state ^{27}Al-NMR spectroscopy has been used to probe the local environments of Al^{3+} centres in LDH-ILs-C12. As is known that the ^{27}Al resonance line positions are very sensitive to the coordination number and are expected to appear within the range of $\delta= -5$ to 15 ppm for octahedral geometry of AlO$_6$ sites.[34] As shown in Fig. 2C, the ^{27}Al-NMR spectrum of LDH-CO$_3$ shows only one peak at $\delta=10.75$ ppm, which clearly demonstrate that all of the Al^{3+} cations in the brucite-like layer adopt octahedral geometry. In the case of LDHs-ILs-C12, the ^{27}Al-MAS-NMR signal shows only one peak with a slight shift to low field chemical shift compared with that of LDH-CO$_3$ (Mg$_3$Al-CO$_3$). This observation indicates that the brucite-like layered structure retains its integrity upon modification of ILs-C12.

BET measurements have been performed on the LDH-ILs-Cn (n=4, 8, 12) samples to obtain more detailed information on the structures of the as-prepared material. As shown in Fig. 2D, taking LDH-ILs-C12 as example, it shows typical type-IV adsorption isotherms, and H3 type hysteresis loops at higher relative pressure ($P/P_0>0.5$), indicating the presence of both interlayer and inter-particle mesopore structures. The pore size distribution calculated by the Barrett-Joyner-Halenda (BJH) method shows a peak centered at around 4.78 nm (Inset Fig. 2D). The specific surface area, pore volume and average pore diameter estimated from N$_2$ adsorption-desorption isotherms of LDH-ILs-Cn (n = 4, 8, 12) are reported in Table S2. SEM images of the as-prepared LDH-ILs-Cn (n=4, 8, 12) show the porous stacking of sheet-like crystallites (Fig. S4). For LDH-ILs-C12, we can see the particle size of these crystallites fall in the range of 1~2 μm.

As shown in Fig. 3, the initial survey of the XPS spectrum shows that the LDH-ILs-C12 sample is composed of Mg, Al C, O, N, Si et al (Fig. 3a). In Fig. 3b-c, the relevant binding energies of Mg 1s and Al 2p can be observed at 1303.6 eV and 77.2 eV, respectively. And Fig. 3d-f exhibit the relevant binding energies of C1s, Si2p, N1s resulting from the modification of the ILs-C12 in the LDH-ILs-C12. In addition, the characteristic peaks for C1s (Fig. 3d) are fitted, in which the three peaks at 284.8 eV (C-C

Table 1. Temperature-programmed desorption of CO_2.

Sample	specific basicity [CO_2 μmol g^{-1}][a]			
	total	w	m	s
LDH-ILs-C4	668	324 (49)[b]	200 (30)	144 (21)
LDH-ILs-C8	672	217 (32)	248 (37)	207 (31)
LDH-ILs-C12	666	243 (36)	137 (21)	286 (43)

[a]w: weak basic sites; m: moderate basic sites; s: strong basic sites. The calculation of the amount of specific basicity using $CaCO_3$ as an internal standard substance and the data was deducted from the decomposition of interlayer of carbonate. [b] Relative amounts of the basic sites (%).

bond) of the alkyl chain, 286.7 eV (C-O bond), and 288.6 eV (O-C=O bond) can be seen.[29] Moreover, in order to detect the electronic state of Si atoms, the Si2p spectra of LDH-ILs-C12 are fitted to two main peaks as shown in Fig. 3e. The Si-O bond at ca.101.7eV can be assigned to the reacted Si-O-M (M=Al or Mg); The Si-C bond at ca. 102.1 eV can be attributed to the silane moieties of ILs-C12.[29] In addition, the Si atoms in Si-OH can be distinguished by fitting program as represented with a weak intensity peak at 103.1 eV. It may be due to the unreacted Si-OH (hydrolysis of the triethoxysilyl group) in the region where is geometrically unavailable.[30,35] This is consistent with the characterization of solid-state ^{29}Si CP/MAS NMR spectrum that shows bidentate and monodentate of Si species. Furthermore, the characteristic peak associated with N1s (Fig. 3f) is centered at 399.7 eV, which can be assigned to the C-N bond of the imidazole rings in ILs-C12.[36] The results provide further support for the covalently grafting ILs-C12 onto the LDH successfully.

Fig. S5a-c presents the Temperature-programmed desorption of CO_2 (CO_2-TPD) curves of LDH-ILs-C4, LDH-ILs-C8 and LDH-ILs-C12, while Fig. S5d is the CO_2-TPD curves of LDH-CO_3 as control experiment. Note that the TCD signals in Fig. S5a-c include the contribution of decomposition of the intercalated carbonate anions. It can be seen that these composites display three kinds of CO_2 desorption peaks, which can be attributed to weak basic sites centered at 90-250 °C, medium basic sites centered at 300-430 °C; and strong basic sites ranging from 500 to 630 °C. The desorption peak of CO_2 in the range of 640-900 °C, which can be assigned to the decomposition of internal standard $CaCO_3$. The data in Table 1 is on the basis of deduction of the CO_2 contribution by the decomposition of the intercalated CO_3^{2-} anions. The results show that the total basic sites remain approximately equal for LDH-ILs-Cn (n = 4, 8, 12).

To have a better understanding of the interactions between the catalyst and reactants under the experimental conditions, the amphiphilic property of the LDH-ILs-Cn (n=4, 8, 12) catalysts has been investigated. As shown in Fig. 4a, when a droplet of water contact the surface of LDH precursor, it forms a contact angle of approximately 29.1°, indicating that the LDH precursor is highly hydrophilic. However, when a water droplet is in contact with the LDH-ILs-Cn (n=4, 8, 12), the contact angles increase with the increase of the alkyl chain length of the modified ILs (Fig. 4b-d). And the hydrophobicity increases according to the following sequence: LDH-ILs-C4 <
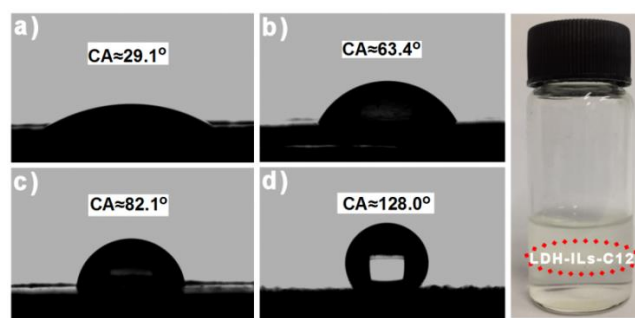

Fig. 4. Water droplets on the surface of the catalyst a) LDH-CO_3, b) LDH-ILs-C4, c) LDH-ILs-C8, d) LDH-ILs-C12. Photographs of LDH-ILs-C12 appeared at the H_2O/organic substrates interface.

LDH-ILs-C8< LDH-ILs-C12. The enhanced hydrophobicity for LDH-ILs-Cn is attributed to the hydrophobic nature of the ILs-Cn. For example, LDH-ILs-C12, exhibits a CA (contact angle) of ca.128°, which is indicative of its increased hydrophobic character compared with LDH precursor. Moreover, the increased hydrophobicity helps the accessibility of the reactants to the catalytic site. For example, the LDH-ILs-C12 can be well dispersed at the interface of the H_2O and organic phases (Fig. 4), which further confirms the amphiphilic nature of LDH-ILs-C12.

3.2. Effect of catalysts on the Knoevenagel condensation

To evaluate the catalytic performance of LDH-ILs-C12, we select the Knoevenagel condensation of benzaldehyde with ethyl cyanoacetate as a model reaction under the experimental conditions (Scheme 1). The reaction proceeds efficiently in water in the presence of a catalytic amount of LDH-ILs-C12 at room temperature and the corresponding product can be obtained in an excellent yield of 99.9 % (entry
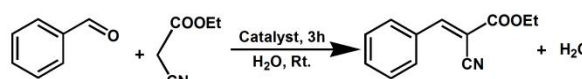
Scheme 1. The Knoevenagel condensation of benzaldehyde with ethyl cyanoacetate.

Table 2 Effect of different catalysts on Knoevenagel condensation of benzaldehyde with ethyl cyanoacetate at room temperature in aqueous solution.[a]

Entry	Catalysts	Yield (%)
1	LDH-ILs-C4	85.1
2	LDH-ILs-C8	84.2
3	LDH-ILs-C12	99.9
4	LDH-CO_3	19.0
5	ILs-C4	30.7
6	ILs-C8	31.4
7	ILs-C12	34.6
8[b]	LDH-CO_3+ILs-C12	45.2
9	None	<1

[a]Reaction conditions: 1 mmol benzaldehyde, 1.5 mmol ethyl cyanoacetate, 30 mg catalyst, 0.5 mL H_2O, 3 h, rt. [b]The catalytic amount of the physical mixture control experiments was used its corresponding individual components load in the composite of LDH-ILs-C12. Yields were determined by GC analysis using reference standards. Assignments of corresponding products were analysed by ^{1}H NMR and ^{13}C NMR spectroscopy in Fig S6.

3). Notably, the excellent catalytic activity of LDH-ILs-C12 may originate from stronger basic sites of LDH-ILs-C12 than those of LDH-ILs-C4 and LDH-ILs-C8. However, almost no yield is obtained in the absence of catalyst (entry 9). In another words, the reaction cannot proceed without catalyst. Application of ILs-C4, ILs-C8 and ILs-C12 to catalyse the reaction at same experiment conditions gives the yields of 30.7%, 31.4%, 34.6%, respectively (entry 5-7). If the unmodified LDH-CO$_3$ is used as a catalyst, the reaction proceeds sluggish with a very low yield of 19.0% (entry 4). Moreover, the reaction shows poor activity using a physical mixture of the individual components of the composite (entry 8). Control experiments (entries 1-2) using LDH-ILs-C4 and LDH-ILs-C8 exhibit inferior catalytic activities to that of LDH-ILs-C12. All the above experimental results in Table 1 indicate the LDH-ILs-C12 is a highly effective catalyst for Knoevenagel reactions. Taking into account the previously reported results and our experimental data discussed herein, the synergistic effect between the LDH layers and the ILs-C12 in the LDH-ILs-C12 is crucial for the efficient promotion of the Knoevenagel reaction.

3.3 Kinetic study of Knoevenagel condensation of benzaldehyde with ethyl cyanoacetate

In an effort to obtain the kinetic parameters for the Knoevenagel condensation of benzaldehyde with ethyl cyanoacetate, control experiments was performed with 1 mmol benzaldehyde, 1.5 mmol ethyl cyanoacetate, and 30 mg LDH-ILs-C12, at room temperature in 0.5 ml H$_2$O conditions. The yield and ln(C_t/C_0) are plotted against the reaction time in Fig. 5A, where C_0 and C_t are the initial corresponding product concentration and corresponding product concentration at time "t", respectively. LDH-ILs-C12 composite shows excellent catalytic activity and the yield can reach 95.6% over 2 h. The linear fit of the data reveals that the catalytic reaction exhibits pseudo-first-order kinetics for the Knoevenagel condensation (R^2=0.994). The rate constant k for the Knoevenagel reaction can be determined to be 0.023 min^{-1} on the basis of Equations (1) and (2). The Knoevenagel reaction of benzaldehyde with ethyl cyanoacetate can be complete with a yield of > 99% in 3h. Thus, the catalyst LDH-ILs-C12 exhibits a high catalytic

Fig. 5. A) Kinetic profiles of the Knoevenagel condensation of benzaldehyde with ethyl cyanoacetate catalyzed by LDH-ILs-C12-1 (red line: yield of corresponding products; blue line: ln(C_t/C_0), data were obtained by carrying out parallel experiments under the same experimental conditions); B) Experiment to prove the nature of heterogeneous catalyst.

$$-dC_t/dt = kC_t \qquad (1)$$

$$\ln(C_t/C_o) = -kt \qquad (2)$$

efficiency for the Knoevenagel condensations, and the catalytic reaction obeys pseudo-first-order kinetics with 99% selectivity. In order to compare the kinetic parameters with different composite materials for Knoevenagel condensation of benzaldehyde with ethyl cyanoacetate, we also investigate the kinetic parameters of LDH-ILs-C4 and LDH-ILs-C8, and they show lower reaction rate compared with LDH-ILs-C12. (Fig. S7-8).

To confirm that the catalyst is true heterogeneous catalyst, the Knoevenagel reaction is performed using LDH-ILs-C12 as the catalyst in water at room temperature. When the yield reaches about 65 % after 30 min, the solid catalyst can be removed from the reaction mixture. The reaction is allowed to proceed under the same conditions. As a result, it shows that no additional conversion of reactant to product can be observed (Fig. 5B). Addition of the catalyst back to the reaction mixture, the reaction continues. Furthermore, elemental analysis of the removed catalyst and the filtrate by ICP-AES shows that the leaching of magnesium and aluminium are about of 0.15 wt.% of the total composition metal ions. And the slight amount of the leached Mg and Al species has not taken a role of catalysis during the hot-filtration test. This result strongly verifies the heterogeneous nature of LDH-ILs-C12.

To demonstrate the wide applicability of the catalytic system, the Knoevenagel reaction of various aldehydes with ethyl cyanoacetate has been carried out in aqueous solution at room temperature. As shown in Table 3, the corresponding products can be obtained in high yields using LDH-ILs-C12 as a heterogeneous catalyst. For example, the aromatic aldehydes (benzaldehyde) can be converted to the corresponding product in good yield of 95.4 (2h) and 99.9 % (3h), respectively (entries 1-2). For methyl-substituted aromatic aldehydes, such as 2-methylbenzaldehyde, 3-methyl-benzaldehyde, and 4-methylbenzaldehyde can all be converted to the corresponding products in high yields of >99.9% (entries 3-5) in 2h. As for the methoxy-substituted aromatic aldehydes including (2-methoxylbenzaldehyde, 3-methoxybenzaldehyde, and 4-methoxybenzaldehyde), the corresponding products can be obtained in high yield of 99.2%, 98.2% and 91.5% (entries 6-8). The above results indicate that the electron-donating group substituted aromatic aldehydes achieve high yields. In the case of the electron-withdrawing group substituted aromatic aldehydes, such as 2-chlorobenzaldehyde, 3-chlorobenzaldehyde, 2-bromobenzaldehyde, 3-bromobenzaldehyde, 4-bromobenzaldehyde, 2-nitrobenzaldehyde, 3-nitrobenzaledhyde, and 4-nitrobenzaldehyde, high yields can be achieved (entries 9-16). The Knoevenagel condensation of 2-thenaldehyde and 2,4-difluorobenzaldehyde can give excellent yields of > 99% and97.3%, respectively (entries 17-18). In terms of the aliphatic aldehydes, the Knoevenagel condensation of heptanal, nonanal and decanal obtain the yield of 92.5 %, 87.1 % and 82.0 %, respectively (entries 19-21). The catalytic activities decrease slightly with the increase of length of the alkyl chains. This may be due to the increased hydrophobicity
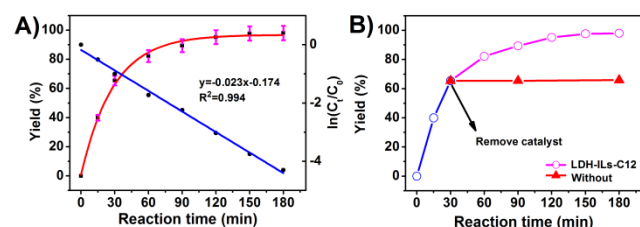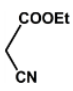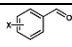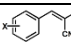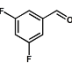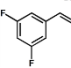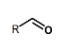
of the substrate. Furthermore, all the resulting products   exhibit over

Table 3 The Knoevenagel condensation of various aldehydes with ethyl cyanoacetate catalysed by LDH-ILs-C12 in aqueous solution at RT[a]

Entry	Donor	Acceptor	Product	Time (h)	Yield[b] (%)	E/Z[c]
1		X=H	X=H	3	99.9	99:1
2				2	95.4	99:1
3		X=2-Me	X=2-Me	2	99.9	99:1
4		X=3-Me	X=3-Me	2	99.9	99:1
5		X=4-Me	X=4-Me	2	99.9	99:1
6		X=2-MeO	X=2-MeO	2	99.2	99:1
7		X=3-MeO	X=3-MeO	2	98.2	99:1
8		X=4-MeO	X=4-MeO	3	91.5	99:1
9		X=2-Cl	X=2-Cl	2	98.9	99:1
10		X=3-Cl	X=3-Cl	2	99.9	99:1
11		X=2-Br	X=2-Br	2	96.3	99:1
12		X=3-Br	X=3-Br	2	99.9	99:1
13		X=4-Br	X=4-Br	2	99.9	99:1
14		X=2-NO$_2$	X=2-NO$_2$	2	99.9	99:1
15		X=3-NO$_2$	X=3-NO$_2$	2	99.9	99:1
16		X=4-NO$_2$	X=4-NO$_2$	2	99.9	99:1
17				2	99.9	99:1
18				2	97.3	99:1
19		R=C$_7$H$_{15}$	R=C$_7$H$_{15}$	2	92.5	99:1
20		R=C$_9$H$_{19}$	R=C$_9$H$_{19}$	2	87.1	99:1
21		R=C$_{10}$H$_{21}$	R=C$_{10}$H$_{21}$	2	82.0	99:1

[a]Reaction conditions: 1 mmol Substrate, 1.5 mmol ethyl cyanoacetate, 30 mg catalyst LDH-ILs-C12, 0.5 mL H$_2$O, rt. [b]Yields were determined by GC analysis using reference standards. Assignments of corresponding products were analyzed by ^{1}H NMR and ^{13}C NMR. [c]E/Z = E isomers of corresponding Knoevenagel condensation products/Z isomers of corresponding Knoevenagel condensation products
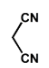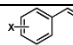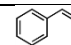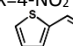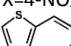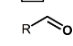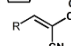
E/Z>99:1. In contrast, the LDH-CO$_3$ precursor shows inferior activity for these aforementioned substrates under same conditions (Table S3).

The catalytic efficiency of the LDH-ILs-C12 composite is evaluated in the Knoevenagel condensation of various aldehydes and ketones with malononitrile in aqueous solution at room temperature. As shown in Table 4, the catalytic performance is excellent for the aromatic aldehyde. This is due to the electron-withdrawing ability of -CN is stronger than that of -COOEt, the methylene group in malononitrile is more active than that in ethyl cyanoacetate. As such, the LDH-ILs-C12 composite can be used for highly efficient catalytic Knoevenagel reaction of various aldehydes with active methylene compounds.

3.4 Comparison with other reported heterogeneous catalysts

The Knoevenagel condensation of ethyl cyanoacetate with benzaldehyde by using different heterogeneous catalysts reported so far is summarized in Table 5. The Knoevenagel condensation reaction by using LDH-ILs-C12 as the catalyst shows its prominent features: 1) excellent catalytic activity can be achieved with the yield of 95.6% in 2 h; 2) the experiments were carried out in aqueous solution at room temperature; 3) high stability and recyclability with a five-run recycling test. In contrast, some other reported catalysts either use toxic and

Table 4 The Knoevenagel condensation of various aldehydes and ketones with malononitrile catalyzed by LDH-ILs-C12 in aqueous solution at RT.[a]

Entry	Donor	Acceptor	Product	t (min)	Yield (%)
1		X=H	X=H	5	99.7
2		X=2-Me	X=2-Me	5	99.9
3		X=3-Me	X=3-Me	5	89.7
4		X=4-Me	X=4-Me	5	99.5
5		X=2-MeO	X=2-MeO	5	89.5
6		X=3-MeO	X=3-MeO	5	98.9
7		X=4-MeO	X=4-MeO	5	99.9
8		X=2-Cl	X=2-Cl	5	91.9
9		X=3-Cl	X=3-Cl	5	91.3
10		X=2-Br	X=2-Br	5	89.6
11		X=3-Br	X=3-Br	5	99.2
12		X=4-Br	X=4-Br	5	92.2
13		X=2-NO$_2$	X=2-NO$_2$	5	95.8
14		X=3-NO$_2$	X=3-NO$_2$	5	97.6
15		X=4-NO$_2$	X=4-NO$_2$	5	99.9
16				5	99.9
17		R=C$_8$H$_{17}$	R=C$_8$H$_{17}$	5	77.6
18		R=C$_9$H$_{19}$	R=C$_9$H$_{19}$	5	87.0
19		R=C$_{10}$H$_{21}$	R=C$_{10}$H$_{21}$	5	81.8

[a]Reaction conditions: 1 mmol Substrate, 1.5 mmol malononitrile, 30 mg catalyst LDH-ILs-C12, 0.5 mL H$_2$O, rt. Yields were determined by GC analysis using reference standards.

Journal Name

Table 5. Various catalytic systems for Knoevenagel condensation of ethyl cyanoacetate with benzaldehyde using different catalysts.

Entry	Catalyst	Ratio[a]	Amount(mg)	Solvent	T [°C]	t [h]	Yield	Ref
1	LDH-ILs-C12	1.5:1	20	water	r.t.	2	95.6	This work
						3	99.9	
2	Aminopropylsily-MCM-41	1.3:1.25	100	toluene	r.t.	1	99	37
3	LaHAP (HAP: Ca10(PO4)6(OH)2)	1.5:1	2mmol%	toluene	60	24	>99	38
4	LDH-F(Mg3Al)	1:1	35	DMF	60	2	92	20
5	LDH-diisopropylamide	2:2	50	DMF	r.t.	2	95	39
6	amine-grafted PE-MCM-41[b]	20:20	45	cyclohexane	82	1	>99.9	40
7	aminopropyl-functionalized MCM	20:20	250	cyclohexane	82	36	94	41
8	aminopropyl-functionalized SBA-15	10:10	150	cyclohexane	82	1	>99	10
9	Organic-inorganic hybrid silica material[c]	1.1:1	1.2mol%	solvent-free	130	2	>99	42
10	Ni–Fe MMO	3:2.5	50	solvent-free	80	8	85	43
11	Mg–Al-In MMO	50:50	1 wt.%	solvent-free	60	24	>99	44
12	Mg–Ga/Al-MMO	50:50	1 wt.%	solvent-free	60	4	82	45
13	Mg3Al-PW12	1.5:1	0.25mol %	2-Propanol/Water	60	6	>99.9	17
14	DMAN/SiO2[d]	7:8	1 mol%	ethanol	60	6	>99.9	46
15	LDH-OH (Mg3Al)	10:10	150	Water	60	10	94	47

Note: [a]Ratio= Ethyl cyanoacetate (mmol)/benzaldehyde (mmol); [b]PE-MCM-41=pore-expanded MCM-41; [c]Organic-inorganic hybrid silica material: containing imidazolium and dihydroimidazolium salts [d]DMAN/SiO2=1,8-bis(dimethylamino)naphthalene-functionalized SiO2.
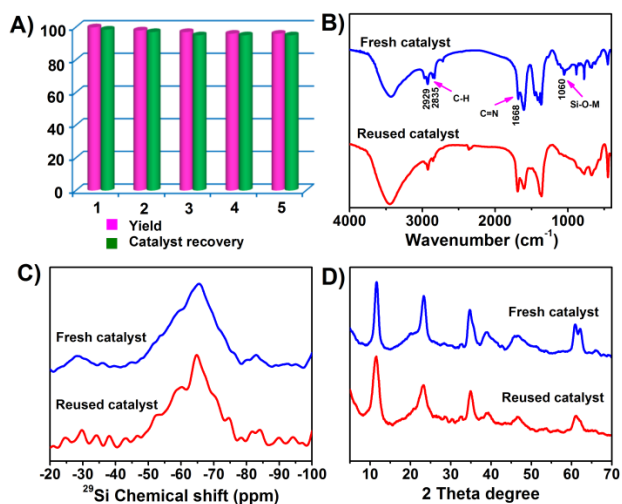

Fig. 6. A) Recycling experiments of LDH-ILs-C12 for the Knoevenagel condensation of benzaldehyde with ethyl cyanoacetate at room temperature in aqueous solution; B) FT-IR spectra; C) solid-state ^{29}Si CP/MAS NMR spectra and D) XRD patterns of the fresh and reused LDH-ILs-C12.

explosive organic solvents (entry 2-8) or suffer from higher reaction temperature (entry 3-4, 6-15). For example, the amine-grafted PE-MCM-41 (entry 6) and aminopropyl-functionalized MCM (entry 7) catalysts require a much higher temperature of 82 °C in cyclohexane to reach a comparable performance; For the catalytic systems of LaHAP (entry 3) and LDH-F (entry 4), toluene and DMF was used as solvents. In the case of organic-inorganic hybrid silica material, a higher temperature (130 °C) was applied to achieve good catalytic results (entry 9).

We have performed a scaled-up experiment by using 50 times of the original experimental conditions (50 mmol benzaldehyde, 75 mmol ethyl cyanoacetate, 1.5 g catalyst, 25 mL H2O, 3 h, rt.). The reaction proceeds smoothly at room temperature in aqueous solution. An excellent yield of benzylidene ethyl cyanoacetate of 96% can be obtained with exclusively *E*-diastereo isomer formed and >99% selectivity. The above experiments demonstrate the LDH-ILs-C12 is an ideal candidate for further application.

3.5 Recycling experiments

Catalyst stability and recyclability is a practical and vital topic for heterogeneous catalysis. Taking the Knoevenagel condensation of benzaldehyde with ethyl cyanoacetate as an example, the recycling experiments having been performed by using LDH-ILs-C12 at room temperature in aqueous solution. After reaction, the solid catalyst was recovered by centrifugation, washed with ethanol, dried and reused for the next run without adding any fresh catalyst. The catalytic reusability for LDH-ILs-C12 in Knoevenagel condensation reaction is measured by five-run tests (Fig. 6A). The results demonstrate a steady reusability without obvious deterioration of its catalytic activity for this heterogeneous catalyst, whilst catalyst recovery is above 96%. In each run, only the corresponding condensation product can be detected and no other byproducts are found. Furthermore, the characterization of reused catalyst using FT-IR spectrum (Fig. 6B), solid-stare ^{29}Si cross-polarization magic-angle spinning (CP/MAS) NMR spectrum (Fig. 6C) and XRD analyses demonstrate the retention of its structural integrity. ICP-AES and elemental analysis of the reused catalyst also reveal that the composition of the reused LDH-ILs-C12 remains the almost same (Table S1).

4. Conclusion

To summarize, we have successfully prepared a series of novel solid base catalysts LDHs-ILs-Cn (n=4, 8, 12), in which ionic liquids is covalently modified onto the layered of LDHs by

adopting an exfoliation/assembly approach. The grafting of ILs-Cn onto LDHs not only helps to adjust the distribution of basic sites, but also induces flexibility to the catalyst and allows easy accessibility of the active centre by the substrates. Application of LDH-ILs-C12 for Knoevenagel condensation of various aldehydes with ethyl cyanoacetate/malononitrile shows an excellent yield, high selectivity, and efficacy in aqueous solution at room temperature. In addition, the LDH-ILs-C12 exhibits excellent structural stability and recyclability. Therefore, this work presents the robust, sustainable, cost-effective and highly efficient heterogeneous base catalytic systems for Knoevenagel condensation transformation.

Acknowledgements

Notes and references

1 L. Zhang, H. Wang, W. Z. Shen, Z. F. Qin, J. G. Wang, W. B. Fan, *J. Catal.* 2016, **344**, 293-302.
2 G. Postole, B. Chowdhury, B. Karmakar, K. Pinki, J. Banerji, A. Auroux, *J. Catal.* 2010, **269**, 110-121.
3 D. Elhamifar, S. Kazempoor, B. Karimi, *Catal. Sci. Technol.* 2016, **6**, 4318-4326.
4 S. Zhao, Y. Chen, Y. F. Song, *Appl. Catal. A: Gen.* 2014, **475**, 140-146.
5 C. I. Ezugwu, B. Mousavi, M. A. Asraf, Z. X. Luo, F. Verpoort, *J. Catal.* 2016, **344**, 445–454.
6 G. Tuci, L. Luconi, A. Rossin, E. Berretti, H. Ba, M. Innocenti, D. Yakhvarov, S. Caporali, C. Pham-Huu, G. Giambastiani, *ACS Appl. Mater. Interfaces.* 2016, **8**, 30099-30106.
7 S. Balalaie, M. Sheikh-Ahmadi, M. Bararjanian, *Catal. Commun.* 2007, **8**, 1724-1728.
8 D. Elhamifar, S. Kazempoor, *J. Mol. Catal. A: Chem.* 2016, **415**, 74-81.
9 M.J. Climent, A. Corma, I. Dominguez, S. Iborra, M.J. Sabater, G. Sastre, *J. Catal.* 2007, **246**, 136-146.
10 X. G. Wang, K. S. K. Lin, J. C. C. Chan, S. Cheng, *J. Phys. Chem. B.* 2005, **109**, 1763-1769.
11 H. K. Min, S. H. Cha, S. B. Hong, *Chem. Commun.* 2013, **49**, 1115-1117.
12 A. R. Burgoyne, R. Meijboom, *Catal. Lett.* 2013, **143**, 563-571.
13 M. Shirotori, S. Nishimura, K. Ebitani, *J. Mater. Chem. A.* 2017, **5**, 6947-6957.
14 G. L. Fan, F. Li, D. G. Evans, X. Duan, *Chem. Soc. Rev.* 2014, **43**, 7040-7066.
15 S. Omwoma, W. Chen, R. Tsunashima, Y. F. Song, *Coord. Chem. Rev.* 2014, **258-259**, 58-71.
16 R. Y. Yang, Y. S. Gao, J. Y. Wang, Q. Wang, *Dalton Trans.* 2014, **43**, 10317-10327.
17 Y. Q. Jia, Y. J. Fang, Y. K. Zhang, H. N. Miras, Y. F. Song, *Chem. Eur. J.* 2015, **21**, 14862-14870.
18 S. Zhao, J. H. Xu, M. Wei, Y. F. Song, *Green Chem.* 2011, **13**, 384-389.
19 Q. Wang, D. O'Hare, *Chem. Rev.* 2012, **112**, 4124-4155.
20 a) B. M. Choudary, M. L. Kantam, V. Neeraja, K. K. Rao, F. Figueras, L. Delmotte, *Green Chem.* 2001, **3**, 257-260; b) Y. Oka, Y. Kuroda, T. Matsuno, K. Kamata, H. Wada, A. Shimojima, K. Kuroda, *Chem. Eur. J.* 2017, **23**, 9362-9368.
21 H. Sven, S. Andrey, S. Carsten, *J. Mol. Eng. Mater.* 2014, **2**, 1440001-1440007.
22 Y. X. Qiao, W. B. Ma, N. Theyssen, C. Chen, Z. S. Hou, *Chem. Rev.* 2017, **117**, 6881-6928.
23 Y. Zhou, G. Q. Chen, Z. Y. Long, J. Wang, *RSC Adv.* 2014, **4**, 42092-42113.
24 a) B. Sarmah, R. Srivastava, *J. Mol. Catal. A: Chem.* 2017, **427**, 62-72; b) C. N. Dai, J. Zhang, C. P. Huang, Z. G. Lei, *Chem. Rev.* 2017, **117**, 6929–6983.
25 T. F. Li, Z. L. Wang, W. Chen, H. N. Miras, Y. F. Song, *Chem. Eur. J.* 2017, **23**, 1069-1077.
26 K. Yamaguchi, C. Yoshida, S. Uchida, N. Mizuno, *J. Am. Chem. Soc.* 2005, **127**, 530-531.
27 Z. P. Xu, H. C. Zeng, *Chem. Mater.* 2001, **13**, 4555-4563.
28 Y. Furukawa, K. Tadanaga, A. Hayashi, M. Tatsumisago. *Solid State Ionics.* 2011, **192**, 185-187.
29 M. V. Reddy, N. T. K. Lien, G. C. S. Reddy, K. T. Lim, Y. T. Jeong, *Green Chem.* 2016, **18**, 4228-4239.
30 Y. Zhang, X. He, J. Ouyang, H. M. Yang, *Sci Rep.* 2013, **3**, 2948.
31 N. Mizuno, K. Yamaguchi, K. Kamata, *Catal. Surv. Asia.* 2011, **15**, 68-79.
32 A. C. Gomes, S. M. Bruno, C. A. Gamelas, A. A. Valente, M. Abrantes, I. S. Goncalves, C. C. Romao M. Pillinger, *Dalton Trans.* 2013, **42**, 8231-8240.
33 M. Sahoo, K.M. Parida, *Appl. Catal. A: Gen.* 2013, **460-461**, 36-45.
34 K. S. W. Sing, D. H. Everett, R. A. W. Haul, L. Moscou, R. A. Pierotti, J. Rouquerol, T. Siemieniewska, *Pure Appl. Chem.* 1985, **57**, 603-620.
35 Y. D. Lei, Z. H. Tang, L. X. Zhu, B. C. Guo, D. M. Jia, *Polymer* 2011, **52**, 1337-1344.
36 F. J. Liu, R. K. Kamat, I. Noshadi, D. Peck, R. S. Parnas, A. Zheng, C. Z. Qi, Y. Lin, *Chem. Commun.* 2013, **49**, 8456-8458.
37 Y. Kubota, Y. Nishizaki, H. Ikeya, M. Saeki, T. Hida,S. Kawazu, M. Yoshida, H. Fujii, Y. Sugi, *Micropor Mesopor Mater.* 2004, **70**, 135-149.
38 K. Mori, M. Oshiba, T. Hara, T. Mizugaki, K. Ebitani, K. Kaneda, *New J. Chem.,* 2006, **30**, 44-52.
39 M. L. Kantam, A. Ravindra, C. V. Reddy, B. Sreedhar,B. M. Choudary, *Adv. Synth. Catal,* 2006, **348**, 569-578.
40 D. D. Das, P. J. E. Harlick, A. Sayari, *Catal Commun.* 2007, **8**, 829-833.
41 D. J. Macquarrie, D. B. Jackson, *Chem. Commun.* 1997, **18**, 1781-1782.
42 M. Trilla, R Pleixats, M. W. C. Man, C. Bied, *Green Chem.,* 2009, **11**, 1815-1820.
43 D. K. Dumbre, T. Mozammel, PR. Selvakannan, S. B. A. Hamid,V. R. Choudhary, S. K. Bhargava, *J. Colloid Interface Sci.* 2015, **441**, 52-58.
44 F. Li, X. Jiang, D. G. Evans, X. Duan, *J. Porous Mater.* 2005, **12**, 55-63.
45 I. Rousselot, C. Taviot-Guého, J.P. Besse, *Int. J. Inorg. Mater.* 1999, **1**, 165-174.
46 E. Gianotti, U. Diaz, S. Coluccia, A. Corma, *Phys. Chem. Chem. Phys.* 2011, **13**, 11702-11709.
47 K. Ebitani, K. Motokura, K. Mori, T. Mizugaki, K Kaneda, *J. Org. Chem.* 2006, **71**, 5440-5447.